Science of the Total Environment 902 (2023) 166062

Contents lists available at ScienceDirect

Science of the Total Environment

journal homepage: www.elsevier.com/locate/scitotenv

Effects of glyphosate exposure on gut–liver axis: Metabolomic and mechanistic analysis in grass carp (*Ctenopharyngodon idellus*)

Biao Yan [a,b,c], Yumiao Sun [a,b], Kaiyu Fu [a,b], Yindan Zhang [a,b], Lei Lei [a,b], Jun Men [d], Yongyong Guo [a], Shengmin Wu [e,*], Jian Han [a,**], Bingsheng Zhou [a]

[a] State Key Laboratory of Freshwater Ecology and Biotechnology, Institute of Hydrobiology, Chinese Academic of Sciences, Wuhan 430072, PR China
[b] University of Chinese Academy of Sciences, Beijing 100049, PR China
[c] Xianning Engineering Research Center for Healthy Environment, Xianning Medical College, Hubei University of Science and Technology, Xianning 437100, PR China
[d] The Analysis and Testing Center of Institute of Hydrobiology, Chinese Academy of Sciences, Wuhan 430072, PR China
[e] Nanjing Institute of Environmental Sciences, Ministry of Ecology and Environment, Nanjing 210042, PR China

HIGHLIGHTS

- Exposure to glyphosate led to higher intestinal accumulation in grass carp.
- Tissue injury in liver and gut and disturbed lipid metabolism were observed.
- Glyphosate declined biosynthesis of bile acids in liver by interfering related genes.
- Gut microbiota dysbiosis disrupted bile acid circulation and induced gut-liver damage.
- Enterohepatic axis dysregulation might contributed to lipid metabolism disorder.

GRAPHICAL ABSTRACT

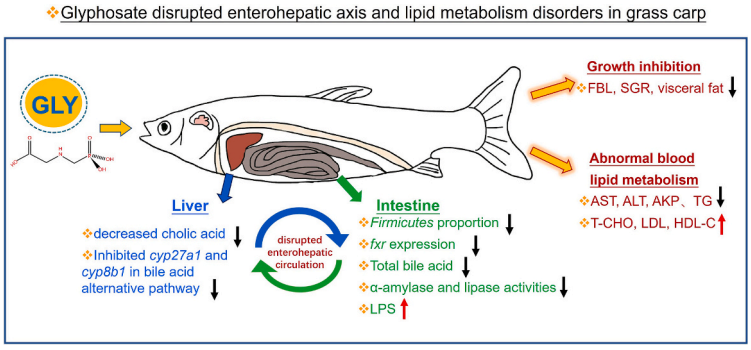

ARTICLE INFO

Editor: Susanne Brander

Keywords:
Glyphosate
Metabolomics
Gut–liver axis
Grass carp

ABSTRACT

Glyphosate, one of the most widely used herbicide worldwide, is potentially harmful to non-target aquatic organisms. However, the environmental health risks regarding impacts on metabolism homeostasis and underlying mechanisms remain unclear. Here we investigated bioaccumulation, metabolism disorders and mechanisms in grass carp after exposure to glyphosate. Higher accumulation of glyphosate and its major metabolite, aminomethylphosphonic acid, in the gut was detected. Intestinal inflammation, barrier damage and hepatic steatosis were caused by glyphosate exposure. Lipid metabolism disorder was confirmed by the decreased triglyceride, increased total cholesterol and lipoproteins in serum and decreased visceral fat. Metabolomics analysis found that glyphosate exposure significantly inhibited bile acids biosynthesis in liver with decreased total bile acids content, which was further supported by significant downregulations of *cyp27a1*, *cyp8b1* and *fxr*. Moreover, the dysbiosis of gut microbiota contributed to the inflammation in liver and gut by increasing lipopolysaccharide, as well as to the declined bile acids circulation by reducing secondary bile acids. These results indicated that exposure to environmental levels of glyphosate generated higher bioaccumulation in gut, where evoked

* Corresponding author.
** Corresponding author at: Institute of Hydrobiology, Chinese Academic of Sciences, No. 7 Donghu South Road, Wuchang District, Wuhan 430072, PR China.
E-mail addresses: wsm@nies.org (S. Wu), hanjian@ihb.ac.cn (J. Han).

https://doi.org/10.1016/j.scitotenv.2023.166062
Received 24 April 2023; Received in revised form 31 July 2023; Accepted 3 August 2023
Available online 4 August 2023

enterohepatic injury, intestinal microbiota dysbiosis and disturbed homeostasis of bile acids metabolism; then the functional dysregulation of the gut-liver axis possibly resulted in ultimate lipid metabolism disorder. These findings highlight the metabolism health risks of glyphosate exposure to fish in aquatic environment.

1. Introduction

Glyphosate, a broad-spectrum herbicide, has been extensively used in terrestrial agricultural system for weed control in agricultural production fields (Van Bruggen et al., 2018). This contributes to the contamination of aquatic system through spray drift, rainwater leaching and agricultural runoff (Villamar-Ayala et al., 2019). In aquaculture, glyphosate is also directly splashed into the water body for control of aquatic weeds and algae in fish ponds (Annett et al., 2014; Van Bruggen et al., 2018; Yan et al., 2022a). In addition, in aquatic ecosystem, glyphosate is often applied in eliminating invasive aquatic plants (Clements et al., 2017). Due to the long-term massive-scale application and high water solubility (Solomon and Thompson, 2003; Zhang et al., 2017), glyphosate has been detected in various water sources in different countries or regions, such as Europe, North America and South America, ranging from 1.80 to 427 μg/L (Van Bruggen et al., 2018). Although glyphosate has been extensively used in China for decades (Zhang et al., 2015), the occurrence and background levels of glyphosate have only recently been reported in China. A large scale environmental survey in 10 provinces of China reported that glyphosate and its major metabolite, aminomethylphosphonic acid (AMPA), were found at maximum levels of 32.5 and 10.3 μg/L in surface water from the agricultural watersheds, respectively (Geng et al., 2021). Our recent study also reported that glyphosate concentrations of 8.89–100 μg/L were detected in freshwater fish ponds from aquaculture basins in Central China, and the highest concentration (267 ng/g·dw) in intestine was found compared with the liver and muscle in grass carp (Yan et al., 2022a). These studies highlight the environmental risks of glyphosate exposure for aquatic organisms.

Increasing evidence have revealed the toxic effects of glyphosate exposure on non-target aquatic organisms, including genotoxicity, neurotoxicity, reproductive toxicity and hepatotoxicity etc. (Agostini et al., 2020; Sabio et al., 2022). Meanwhile, the adverse effects of glyphosate exposure have also been frequently reported in fish species, including oxidative stress, liver damage, inflammatory response, apoptosis (Dey et al., 2016; Shiogiri et al., 2012; Szarek et al., 2000; Zheng et al., 2021), and changes in acetylcholinesterase activity (Glusczak et al., 2006). Notably, studies have demonstrated the disruptions of hepatic nucleotide metabolism (Li et al., 2017; Giommi et al., 2022), hepatic lipid metabolism (Liu et al., 2021), and gut microbiota (Chen et al., 2022) caused by glyphosate exposure. These findings suggest that glyphosate exposure may cause metabolic disorders and adverse health effects involving liver and gut.

The gut is the organ of glyphosate absorption (ATSDR, 2020) and the liver is its major metabolic organ, and the gut-liver axis plays essential role in maintaining metabolic homeostasis of the body (Campana et al., 2022; Evariste et al., 2019). However, it remains unclear whether glyphosate exposure at environmental concentrations could adversely affect the gut-liver axis in fish. Herein, a widely distributed commercial freshwater fish grass carp was exposed to environmentally relevant levels of glyphosate to (1) investigate the effects of glyphosate exposure on the gut-liver axis by using metabolomic and mechanistic analyses, (2) explore the lipid metabolism alterations affected by the gut-liver axis. This study provides novel insights into the toxic profiles of metabolism disruption, with a focus on the environmental health risks of glyphosate to non-target organisms.

2. Materials and methods

2.1. Chemicals

Glyphosate (CAS: 1071-83-6, purity 99.0 %) and AMPA (CAS: 1066-51-9, 98.0 %) were purchased from Sigma-Aldrich (St. Louis, MO, USA). The $^{13}C,^{15}N$-glyphosate (CAS: 1185107-63-4, 99.2 %) and 9-fluorenymethylchloroformate (FMOC-Cl, CAS: 28920-43-6, 98 %) was obtained from Toronto Research Chemicals Inc. (North York, Canada) and Aladdin (Shanghai, China), respectively. The stock solutions of glyphosate were prepared with the double distilled water. Other chemicals were of analytical grade.

2.2. Fish maintenance and exposure

The 25-day-old juvenile grass carp (*Ctenopharyngodon idellus*) (length 4.42 ± 0.02 cm, weight 1.55 ± 0.01 g) were provided by Honghu local aquaculture station, China. Before exposure experiment, the fish were acclimated for 2 weeks in a 250 L glass tank with dechlorinated and aerated water (temperature: 26 ± 1 °C, pH: 7.2–7.5, dissolved oxygen: 6.50 ± 0.5 mg/L) under a 12 h light /12 h dark photoperiod.

Grass carp were randomly selected and exposed to 0, 1, 10 and 100 μg/L glyphosate for 14 days. The exposure concentrations were chosen according to the environmental concentrations in freshwater aquaculture ponds (Yan et al., 2022a). Each exposure group included three replicate tanks (20 L), and each tank contained 20 fish. During the exposure, half of the water was replaced every 24 h, and the fish were fed with commercial diets twice a day. At the end of exposure period, the fish were randomly selected, and euthanized with 300 mg/L MS-222 (Sigma-Aldrich, USA). The weight and length were recorded, where the weight gain rate (WGR, %), specific growth rate (SGR, %/d) were determined. Samples of blood, brain, liver, and intestines (midgut and hindgut) were collected and preserved at −80 °C for subsequent analyses. The grass carp experiments were performed in accordance with the Guidelines for the Care and Use of Laboratory Animals of the Institute of Hydrobiology, Chinese Academy of Sciences.

2.3. Chemical analyses of glyphosate and AMPA

Quantification of glyphosate and AMPA in exposure solutions and organs (brain, liver, intestine and muscle) were performed according to the previous methods (Yan et al., 2022a). Briefly, water (n = 3) and tissue samples (n = 3) were collected and pretreated separately, and then followed by derivatization with fluorenylmethyl chloroformate (FMOC-Cl) combined with solid phase extraction. The $^{13}C,^{15}N$-glyphosate was as an internal standard. The prepared samples were analyzed on a UPLC-MS/MS (Acquity™ UPLC/Xevo TQ MS, Waters, USA), which coupled with a C18 column (2.1 mm × 50 mm × 1.7 μm, Acquity, Waters, USA). The recoveries were 72–106 % for glyphosate and AMPA for 72–99 %, respectively.

2.4. Histological examination and body fat analysis by Micro-CT

Three randomly selected grass carp from each group (n = 3) were anaesthetized for fixation visceral fat scanning on a micro-CT scanner (Skyscan 1276, Bruker, Belgium) according to the previous method (Zhou et al., 2021). Fat tissues were photographed and reconstructed by using the SkyScan CT Vox software (Version 2.3.0) for 3D volume-rendered images (Sakashita et al., 2019). Total adipose tissue volume (TAT), tissue volume (TV) and visceral fat ratio (TAT/TV × 100 %) were

recorded and calculated, respectively.

The liver and intestine tissues of grass carp (n = 3) were fixed in 4 % paraformaldehyde, then dehydrated and embedded in paraffin, and subsequently sliced into 5 μm thickness for hematoxylin-eosin staining. These sections were analyzed by automatic digital slide scanner (Aperio VERSA 8, Leica) for observation and histopathological analysis.

2.5. Hepatic metabolomics analysis

Livers from three groups of 0, 10 and 100 μL were collected for Quasi-targeted metabolomics (Li et al., 2017). Three fish (one per each repeat tank) were pooled as one sample, and five samples of each group were used for following analysis. Liver samples (100 mg) were individually grounded with liquid nitrogen and the homogenate was extracted with prechilled 80 % methanol by well vortex. The extracts were aliquoted, dried under nitrogen, and reconstituted in appropriate solvents containing internal standards, then analyzed using HPLC-MS/MS. HPLC-MS/MS analyses were performed using an ExionLC™ AD system (SCIEX) coupled with a QTRAP® 6500^{+} mass spectrometer. High-resolution full-scan MS data were acquired using positive/negative polarity mode electrospray ionization. The Q1/Q3 (ion pair), RT (retention time), DP (declustering potential) and CE (collision energy) were used to the metabolite identification. The data files generated by HPLC-MS/MS were processed using the SCIEX OS Version 1.4 to integrate and correct the peak. The area of each peak represents the relative quantitative value of the corresponding metabolite. The main databases for pathway and taxonomic annotation of the identified metabolites include KEGG, Human metabolome database (HMDB), LIPID MAPS, etc. The identified metabolites were annotated by using these databases to understand the functional properties and classification of different metabolites. Detailed performance of metabolites extraction, identification and LC-MS chromatographic conditions were presented in supporting information (Text S1).

2.6. Biological determination of metabolic-related parameters

The serum activities for alanine aminotransferase (ALT), aspartate aminotransferase (AST), alkaline phosphatase (AKP), concentrations for triglyceride (TG), total cholesterol (T-CHO), low-density lipoprotein cholesterol (LDL-C), high-density lipoprotein cholesterol (HDL-C) and glucose (GLU) were determined by with commercial test kits (Jiancheng Bio-Engineering Institute, Nanjing, China). Hepatic and intestine contents of total bile acids (TBA) were determined by commercial kits (Nanjing Jiancheng, China). The intestine contents of lipopolysaccharide (LPS) were detected by ELISA kit (Shanghai enzyme-linked, China), and the activities of α-amylase and lipase were detected by commercial kits (Nanjing Jiancheng, China). Protein concentration of the sample was determined with BCA protein analysis kit (Beyotime, China). All determinations were carried out following the manufacturers' protocols.

2.7. Quantitative real-time PCR assays

The livers or intestines of each group were pooled as one sample (n = 3) for total RNA extraction and purification, cDNA synthesis and real-time fluorescence quantitative qRT-PCR. The primer sequences related to bile acids synthesis (e.g., *cyp7a1*, *cyp8b1*, *cyp27a1*, *fxr*, *fgf15*, *hmgcr*) and inflammatory cytokines (e.g., *il-1β*, *il-6*, *tgf-β2* and *tnf-α*) in grass carp are shown in supporting information (Text S2, Table S2 and S3). The relative transcriptional changes of the target genes were calculated by normalizing to *β-actin* with the $2^{-\Delta\Delta Ct}$ method.

2.8. Gut microbiota analysis

Intestines (n = 3, 5 fish intestines pooled as one sample) were used for 16S rRNA gene amplicons sequencing. In brief, genomic DNA was isolated from approximately100 mg of each sample by using a DNA extraction kit (QIAamp®, Qiagen Ltd., Germany). The primers (338F: 5′-ACTCCTACGGGAGGCAGCA-3′ and 806R: 5′-GGACTACHVGGGTWTC-TAAT-3′) were used to amplify the V3-V4 region of the 16S rRNA gene (Zhou et al., 2018). The amplified products were purified and quantified, and then constructed amplicon libraries for subsequent sequencing on the Illumina MiSeq-PE25 platform (Illumina, USA). The operational taxonomic units (OTUs) with a 97 % homology threshold were clustered by using QIIME 1.9.1 (OTU sequence similarity: 0.97 taxonomic confidence, 0.7 taxonomic database: 16S, Silva138/16S_bacteria; Shanghai Majorbio cloud platform).

2.9. Statistical analysis

GraphPad Prism 8.02 (GraphPad, USA) was used to generate statistical figures, and values were showed as mean ± standard deviation (Mean ± SD). Before analysis, all data were tested for normality and homogeneity with Shapiro-Wilk test and Levene's test, respectively. The difference between the control and treated groups was then analyzed by one-way analysis of variance (ANOVA) with post hoc pairwise comparisons, and was determined as statistically significant with $p < 0.05$. The Kruskal-Wallis H test was performed to analyze the differences in gut microbial diversity among all groups. Metabolomics data were statistically analyzed using NovoMagic cloud platform, including univariate (Tukey test and *t*-test) and multivariate (PCA and OPLS-DA) analysis. KEGG (https://www.genome.jp/kegg/pathway.html), HMDB (https://hmdb.ca/metabolites) and LIPID Maps (http://www.lipidmaps.org/) were used to annotate the identified metabolites. MetOrigin, a free available web tool (http://metorigin.met-bioinformatics.cn/) was used to discriminate the origins of microbial metabolites for integrative analysis of the gut microbiome and metabolome.

3. Results

3.1. Detection of glyphosate in water and tissues

The measured concentrations of glyphosate in the exposure solutions just after renewal were 1.06 ± 0.07, 9.64 ± 0.26 and 98.30 ± 5.58 μg/L in 1, 10 and 100 μg/L groups, respectively. After 24 h, the measured concentrations were 0.63 ± 0.04, 7.13 ± 0.49 and 67.00 ± 3.85 μg/L in the corresponding groups, respectively.

The glyphosate and AMPA were measured in liver, gut, brain and muscle, and the contents showed a dose-dependent manner (Fig. 1). Specifically, the measured concentrations for glyphosate and AMPA in intestine were the highest, followed by liver and muscle, while small amount of glyphosate was also measured in brain. The concentrations in the control tanks or control fish were below the limit of detection.

3.2. Effects of glyphosate exposure on growth and fat composition

There were no malformations or mortalities during exposure period. However, exposure to 10 and 100 μg/L glyphosate significantly decreased in body length, weight gain rate (WGR, %) and specific growth rate (SGR, %/d) (Fig. 2A–C). The body weight and hepatosomatic index (HSI, %) was not changed (Fig. S2).

The visceral fat of grass carp decreased gradually with the increasing glyphosate exposure concentration, and showed a significant difference between the control and 100 μg/L groups (Fig. 2E–F).

In serum, the contents of TG were significantly decreased at 10 and 100 μg/L exposure groups, while the concentrations of T-CHO and LDL-C were decreased at 100 μg/L, HDL-C was also increased in 10 and 100 μg/L (Table 1). No significant difference was observed in GLU (Table 1).

3.3. Histopathological, biochemical measurement and inflammation

In the liver, histological examination observed that glyphosate exposure caused cytoplasmic vacuolization, pyknotic and lost nucleus in

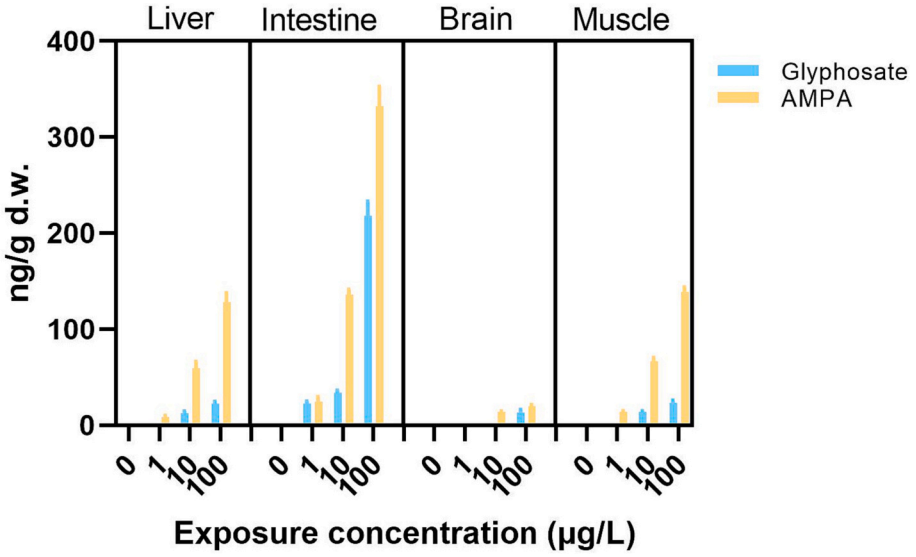

Fig. 1. The contents of glyphosate and AMPA in the liver, intestine, brain and muscle of grass carp after exposure to glyphosate for 14 days (ng/g·dw; $n = 3$). AMPA, aminomethylphosphonic acid.

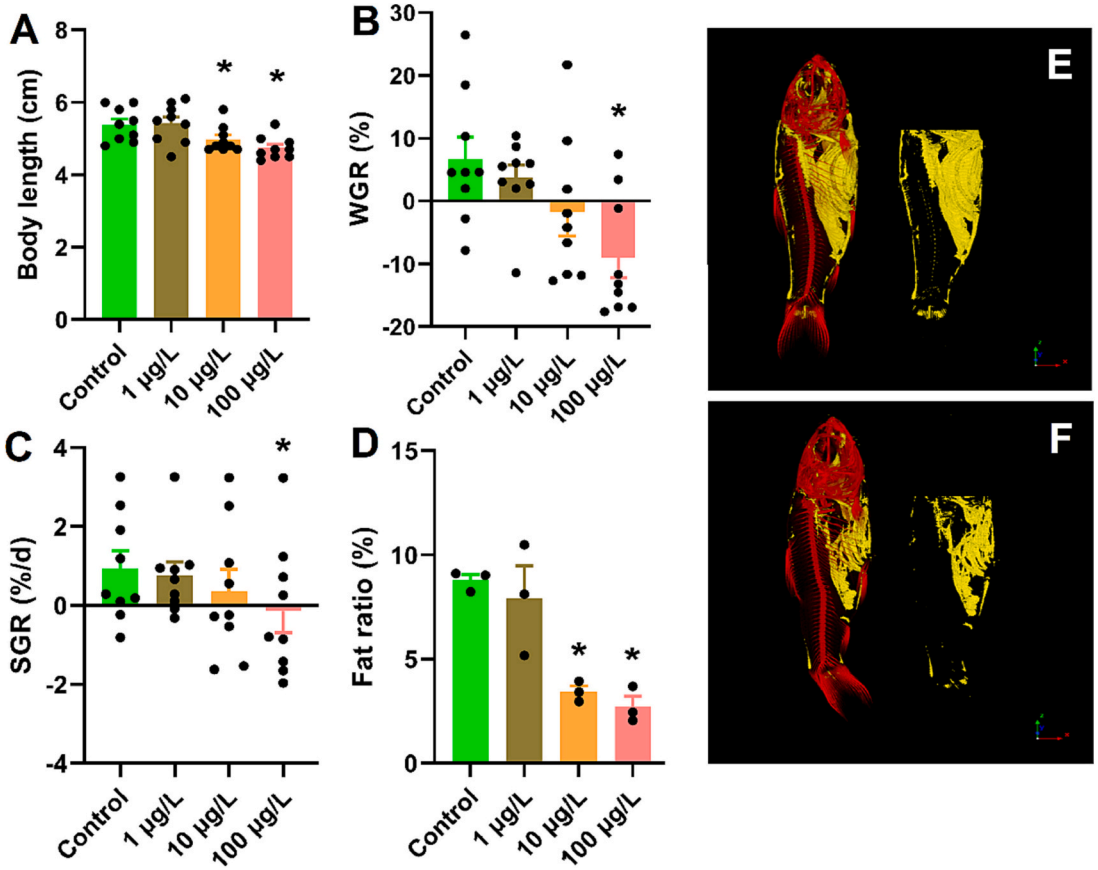

Fig. 2. Growth performance and fat composition in grass carp after exposure to glyphosate. A, body length; B, weight gain rate (WGR); C, specific growth rate (SGR); D, fat ratio; E and F, visceral fat composition (red, bone skeleton; yellow, fat) in the Control and 100 μg/L groups, respectively. A-C, $n = 9$; D–F, $n = 3$. *$p < 0.05$.

hepatocytes (Fig. 3B). In the gut, glyphosate exposure damaged the intestinal basement membranes, resulting in the lamina propria, striate margin and villus defect were observed (Fig. 3D).

In serum, the ALT, AST and AKP activities were significantly decreased with a dose-dependent manner (Table 2). In the gut, the concentrations of LPS were significantly increased, while the activities of both α-amylase and lipase were decreased in 10 and 100 μg/L groups (Table 2).

For the transcriptions of inflammation related genes in liver and intestine. In the liver, a dose-dependent upregulations of *il-1β*, *il-6*, *tgf-β2* and *tnf-α* were observed and showed significant difference in 100 μg/L group (Fig. 3E). Likewise, upregulation of those gene expressions was

Table 1
Changes of serum biochemical parameters in grass carp after exposure to glyphosate. TG, triglyceride; T-CHO, total cholesterol; LDL-C, low-density lipoprotein cholesterol; HDL-C, high-density lipoprotein cholesterol; GLU, glucose. (n = 3. *$p < 0.05$, **$p < 0.01$).

Indices (mmol/L)	Control	1 μg/L	10 μg/L	100 μg/L
TG	4.84 ± 2.24	5.41 ± 2.73	2.23 ± 1.15	1.66 ± 1.23
T-CHO	1.86 ± 0.82	2.54 ± 1.10	2.86 ± 0.78	3.56 ± 0.86 **
LDL-C	0.13 ± 0.08	0.08 ± 0.10	0.21 ± 0.05	0.26 ± 0.06 **
HDL-C	0.19 ± 0.19	0.24 ± 0.14	0.48 ± 0.15 *	0.49 ± 0.10 **
GLU	1.28 ± 0.93	1.41 ± 0.63	1.23 ± 0.71	0.86 ± 0.65

also measured in the intestine, among them, the *tgf-β2* gene transcriptions were upregulated at all exposure concentrations (Fig. 3F).

3.4. Hepatic metabolomics changes

3.4.1. Differences in hepatic metabolites and perturbed pathways

The model was reliably established by orthogonal partial least squares discriminant analysis (OPLS-DA), liver tissues from the glyphosate-exposed groups were clearly separated from tissues from the controls (Fig. S3, Text S3). The total number of metabolites identified by hepatic metabolomics was 733. There were 37 differential metabolites significantly down-regulated and 9 differential metabolites significantly up-regulated in the 10 μg/L group compared with the control, and 40 differential metabolites significantly down-regulated and 5 differential metabolites significantly up-regulated in the 100 μg/L group compared with the control (Table S4, Fig. S4). Among them, 78 different lipids were identified, mainly including 24 fatty acids and conjugates, 25 sterol lipids (e.g., taurine, TLCA, TCA, TCDCA, CDCA, TUDCA, TDCA, THCA). The classification, annotation and pathway enrichment analysis on identified metabolites revealed that the metabolism processes were the mainly affected pathways (Fig. S5a). Considering the suspected steatosis in liver, the differential metabolites were further annotated by running against the two main databases, the KEGG and LIPID MAPS, and showed that the bile acids metabolism was of the most affected pathway (Fig. S5b and c). Among the identified eight bile acids metabolites, only taurine and TLCA were slightly increased, and the other six were significantly decreased in the 100 μg/L group (Fig. 4A). Notably, the relative cholic acids in the 100 μg/L group was lower than that in control (Fig. 4B). There was a significantly decreasing trend of total hepatic bile acids content (Fig. 4C). In the gut, the measured bile acids content in the 10 and 100 μg/L group were significantly decreased (Fig. 4D).

3.4.2. Expression levels of bile acids synthetic genes in liver and gut

For further confirmation of the pathway evoked by exposure to glyphosate in the liver, several key genes related to bile acids metabolism pathway were detected. The mRNA expression of *cyp27a1* and *cyp8b1* in the conversion from cholesterol (7α-hydroxycholesterol, 27-hydroxycholesterol) to cholic acid (CA) were significantly down-regulated in 10 and 100 μg/L treatment groups (Fig. 4E). The primary bile acids biosynthesis pathway (map00120) regulated by these two genes are shown in Fig. S6. The *hmgcr* and *fxr* gene transcriptions were

Table 2
The activities of alanine aminotransferase (ALT, U/L), aspartate aminotransferase (AST, U/L) and alkaline phosphatase (AKP, U/L) in serum, and α-Amylase (U/mg protein) and Lipase (U/g protein) in gut of grass carp after exposure to glyphosate. In addition, lipopolysaccharide (LPS, ng/mg protein) was also determined in gut. (n = 3. *$p < 0.05$, **$p < 0.01$).

Indices	Control	1 μg/L	10 μg/L	100 μg/L
ALT	42.10 ± 5.35	33.90 ± 11.70	23.50 ± 7.43 *	9.96 ± 2.82 **
AST	150.70 ± 35.20	57.20 ± 12.40 **	46.90 ± 13.50 **	8.27 ± 1.50 **
AKP	504.90 ± 102.10	76.90 ± 38.80 **	75.50 ± 10.74 **	53.00 ± 27.90 **
α-Amylase	0.98 ± 0.09	0.90 ± 0.04	0.83 ± 0.09 *	0.82 ± 0.04 *
Lipase	4.97 ± 2.35	2.55 ± 0.70	2.32 ± 0.66 *	2.26 ± 0.77 *
LPS	28.90 ± 9.62	37.70 ± 24.20	47.50 ± 13.20 *	48.90 ± 19.60 *

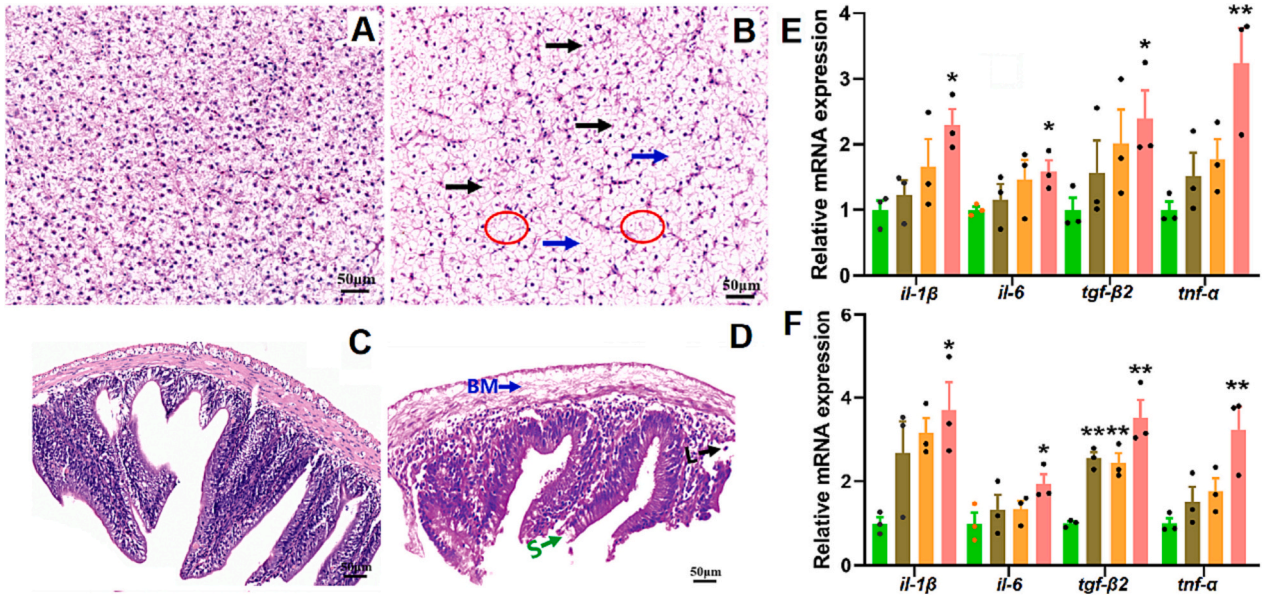

Fig. 3. Histopathological, biochemical and immune changes in the liver and intestine. A and B, livers from the control and 100 μg/L group, respectively; blue arrow indicates vacuolization, black arrow indicates pyknotic nucleus, and areas in red ellipses indicate cells without nucleus. C and D, intestines from the control and 100 μg/L group, respectively; blue arrow indicates basement membrane damage (BM), black arrow indicates lamina propria lost (L), and green arrow indicates striate margin and villus defect (S). E and F indicate transcriptional changes of inflammation related genes in liver and intestine, respectively. $n = 3$. *$p < 0.05$, **$p < 0.01$. *il-1β*, interleukin 1 β; *il-6*, interleukin 6; *tgf-β2*, transforming growth factor β2; *tnf-α*, tumor necrosis factor α.

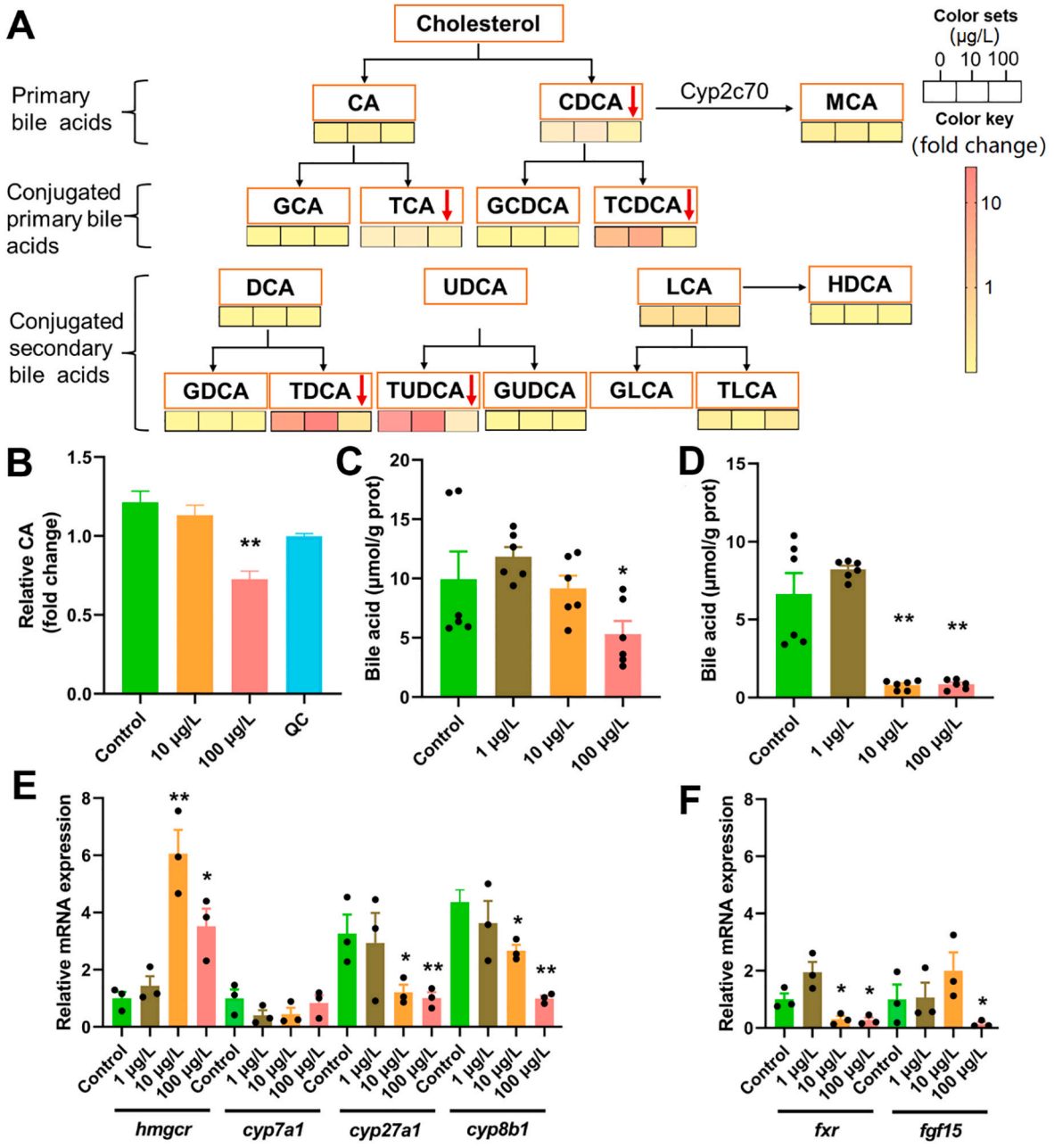

Fig. 4. Bile acids metabolism in liver and intestine of grass carp after exposure to glyphosate. A, the identified differential bile acids metabolites; Color sets indicates the exposure concentration, and color keys indicates the fold change. B, the relative cholic acid (CA). The default criteria for differential metabolites identified were VIP > 1.0, FC > 1.5 or FC < 0.667, $p < 0.05$; Quality control (QC). C, total bile acids contents in liver. D, total bile acids contents in intestine. E, expression levels of bile acids synthetic genes in liver. F, expression level of genes related to bile acids signal pathway in intestine. A–B, $n = 5$; C–D, $n = 6$; E–F, $n = 3$. *$p < 0.05$, **$p < 0.01$. CA, Cholic acid; CDCA, Chenodeoxycholic acid; GCA, Glycocholic acid; TCA, Taurocholic acid; GCDCA, Glycochenodeoxycholic acid; TCDCA, Taurochenodeoxycholic acid; DCA, Deoxycholic acid; UDCA, Ursodeoxycholic acid; LCA, Lithocholic acid; HDCA, Hydroxycholic acid; GDCA, Glycodeoxycholic acid; TDCA, Taurodeoxycholic acid; TUDCA, Tauroursodeoxycholic acid; GUDCA, Glycoursodeoxycholic acid; GLCA, Glycolithocholic acid; TLCA, Taurolithocholic acid. *cyp7a1*, cholesterol 7α-hydroxylase; *cyp7b1*, oxysterol 7α-hydroxylase; *cyp8b1*, sterol 12α-hydroxylase; *cyp27a1*, sterol 27-hydroxylase; *hmgcr*, 3-hydroxy-3-methylglutaryl-CoA reductase; *fgf15*, fibroblast growth factors 15; *fxr*, farnesoid X receptor.

up-regulated in 10 and 100 μg/L groups (Fig. 4E). In the intestine, *fxr* gene transcriptions were strongly inhibited in 10 and 100 μg/L groups, while a marked downregulation of *fgf15* gene transcription was observed in 100 μg/L group (Fig. 4F).

3.5. Changes in composition of gut microbiota

Based on 16S rRNA sequencing performed on intestinal microbiota, community richness of gut microbiota in exposed grass carp, were deviated from the control group (Fig. 5A and C). In grass carp exposed to glyphosate, 100 g/L glyphosate significantly increased Shannon and decreased Simpson indices ($p < 0.05$), and resulted in a significantly changed gut microbiota (Fig. S7, Text S4). The dominant genera at the phylum level in fish gut were: Proteobacteria, Actinobacteriota, Firmicutes, Fusobacteria, Spirochaetota, Bacteroidota, etc. (Fig. 5B). Among them, the proportion of Proteobacteria in the 100 μg/L group was 59.19 %, which was much higher than that in the control (24.54 %). Firmicutes accounted for 9.22 %, much lower than the control (20.3 %). The

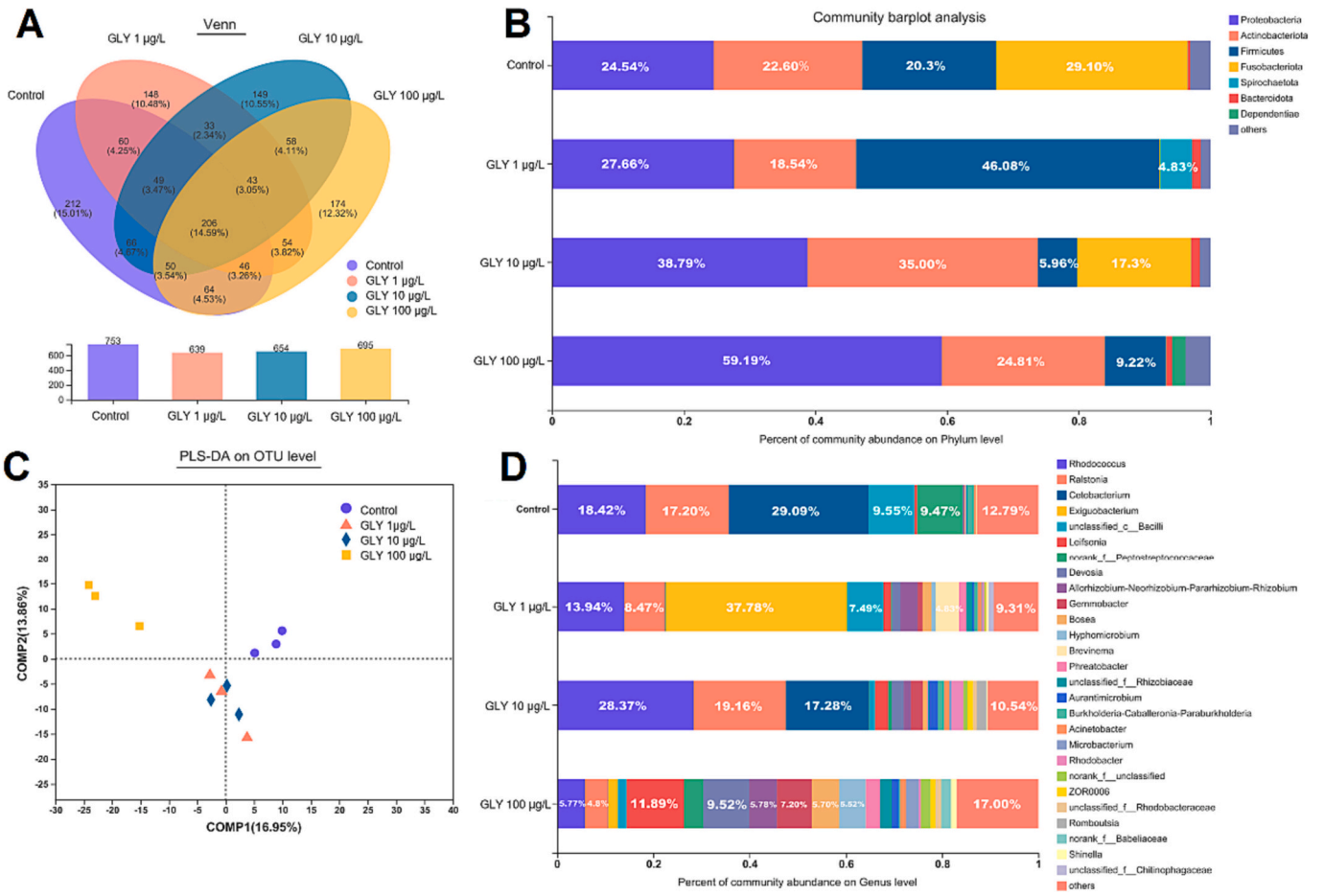

Fig. 5. Differences in gut microbial community composition of grass carp exposed to glyphosate (GLY) ($n = 3$). A, OTU Venn diagram; C, PLS-DA analysis, B and D, differences in microbial community composition at phylum level and at genus level, respectively.

relative abundances of the phylum of Proteobacteria were significantly enriched in 100 μg/L group, while an opposite change of Firmicutes was also observed (Fig. S8). At the genus level, the dominant genera were: *Rhodococcus*, *Ralstonia*, *Acetobacterium*, *Cetobacterium*, *Exiguobacterium*, *Leifsonia*, etc. Among them, the proportion of *Rhodococcus* in 100 μg/L group was 5.77 %, which was much lower than that in the control (18.42 %) (Fig. 5D).

3.6. Correlations of liver metabolites, biochemical and growth indices with gut microbiota

The hepatic metabolites from different sources (host or microbiota) were identified with MetOrigin analysis, 483 metabolites classified into 4 categories: 16 metabolites of host origin, 66 metabolites of microbiota origin, 236 metabolites of co-metabolism shared between microbiota and host, and 165 metabolites of other sources (drugs or food, etc.) (Fig. 6A). These differential metabolites were selected according to the different source for enrichment pathway analysis, and were enriched into lipid metabolic pathways (Fig. 6B). Specifically, among the common metabolic pathways, the metabolites related to fatty acids and primary bile acids biosynthesis were significantly enriched. The canonical correlation analysis (CCA) revealed that gut microbiota was negatively correlated with growth-related parameters (FBL, SGR, WGR) and biochemical parameters (AST, AKP, ALT, TG) in 100 μ/L group (Fig. 6C), but positively correlated with biochemical parameters (T-CHO, LDL-C, HDL-C). The correlation among differential genera, growth parameters and biochemical parameters was visually evaluated by Spearman correlation analysis (Fig. 6D). These results revealed that seven kinds of differential genera (*Microbacterium*, *unclassified_f_Rhodobacteraceae*, *Aurantimicrobium*, *Bosea*, *Gemmobacter*, *Devosia*, *Leifsonia*) were negatively correlated with growth parameters (FBL). Nine kinds of differential genera (*unclassified_f_Rhodobacteraceae*, *norank_f_unclassified*, *Microbacterium*, *Rhodobacter*, *Aurantimicrobium*, *Bosea*, *Gemmobacter*, *Devosia*, *Leifsonia*) were negatively correlated with biochemical parameters (ALT, AST and AKP).

4. Discussion

In the present study, we investigated the effects of glyphosate exposure on juvenile grass carp metabolism and health risks at environmental realistic concentrations. Glyphosate exposure had several negative effects on grass carp, including reduced growth, pathological damage and inflammation in the liver and intestine, reduced liver function, and increased blood lipid levels. Exposure to glyphosate also disrupted the physiological functions of the intestinal flora, diminished the Firmicutes genera, and inhibited intestinal *fxr* and *fgf15* genes expression, resulting in inhibition of bile acids synthesis in the liver. Moreover, glyphosate exposure reduced hepatic *cyp27a1* and *cyp8b1* genes expression, which suppressed the conversion of cholesterol to bile acids, leading to a decrease in total bile acids in the liver and intestine. These effects ultimately disrupted lipid metabolism and growth in the exposed fish, highlighting the health hazards of environmental levels of glyphosate exposure to aquatic vertebrates.

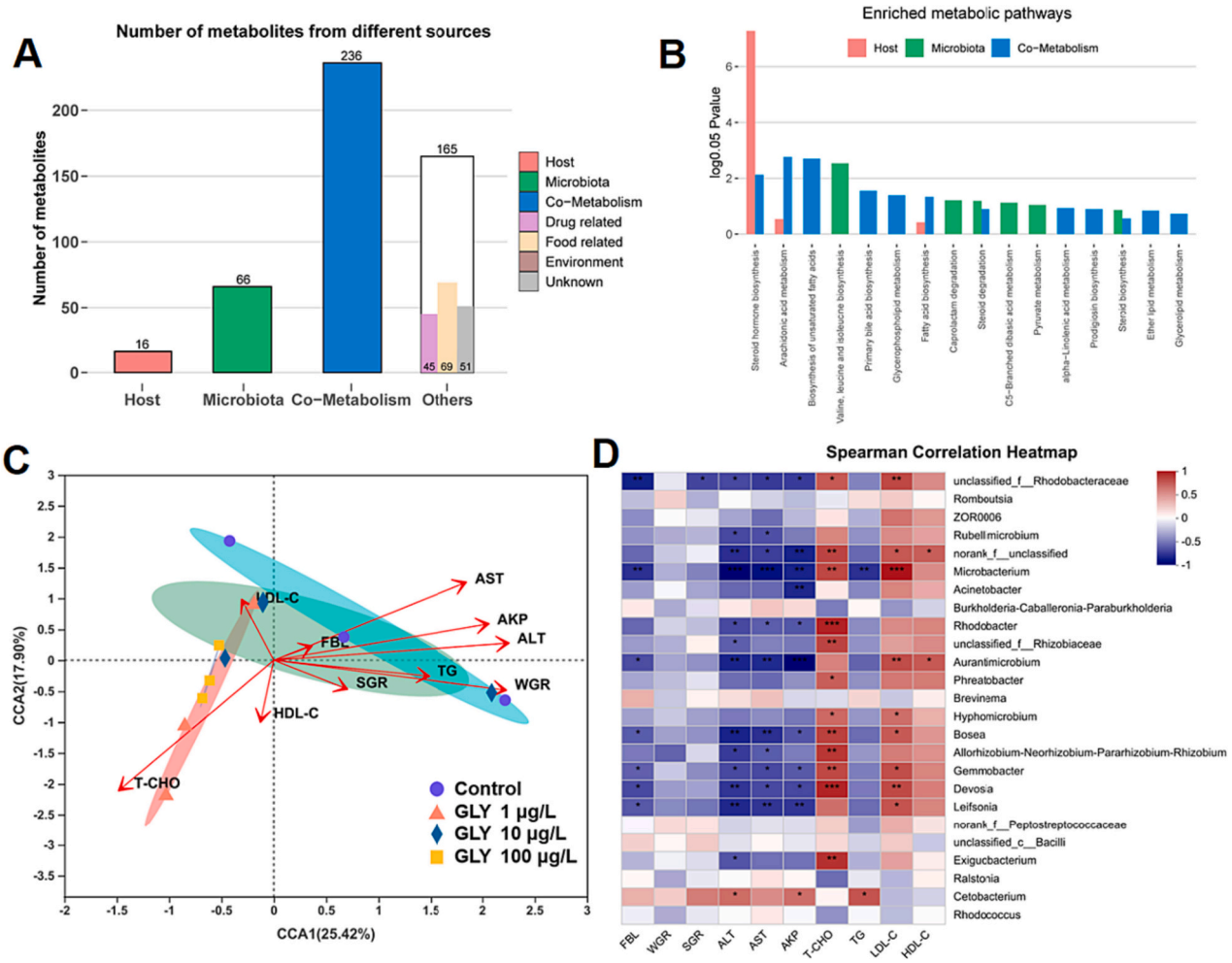

Fig. 6. Original identification and metabolic pathway enrichment of liver metabolites, and correlation analysis among growth indices, biochemical indices and specific gut microbiota composition. A, number of metabolites from different sources. B, enriched metabolic pathways. C, canonical correlation analysis (CCA) analysis on the correlations between the differential growth parameters (FBL, SGR, WGR) and biochemical parameters (ALT, AST, AKP, T-CHO, TG, LDL-C, HDL-C). D, spearman correlation analysis; red and blue colors indicated negative and positive correlations, respectively. The significance of correlation was denoted by stars ($p < 0.05$, with $r > 0.5$ or < -0.5). GLY, glyphosate; FBL, final body length; WGR, weight gain rate; SGR, specific growth rate; ALT, alanine aminotransferase; AST, aspartate aminotransferase; AKP, alkaline phosphatase; TG, triglyceride; T-CHO, total cholesterol; LDL-C, low-density lipoprotein cholesterol; HDL-C, high-density lipoprotein cholesterol.

4.1. Bioaccumulation of glyphosate

Chemical analysis showed fish intestine enriched higher contents of glyphosate and AMPA than those in liver, brain and muscle. Moreover, the content of AMPA was higher than its parental compound, indicating that glyphosate is readily metabolized. The results are consistent with our previous field study, showing that the concentration of glyphosate was lower than AMPA in tissues, while intestine concentrations were higher than those other tissues in grass carp (Yan et al., 2022a). The result also suggests that in addition to liver, intestine might also be a major target organ for glyphosate bioconcentration and metabolism. It has been reported that tissues with a lower metabolic rate, such as muscle, have a lower bioaccumulation potential (Fantón et al., 2021). Hence, the organs with potent metabolic activities, like liver and intestine, can bioaccumulate higher levels of glyphosate than brain and muscle.

4.2. Histopathology and inflammatory responses

Histopathological examination observed changes including cytoplasmic vacuolization and pyknotic nucleus, but liver injury parameters, such as ALT, AST and AKP were not increased in serum. The present study contrasts with several previous studies, showing that apparent histopathological changes, including swelling of hepatocytes, severe cytoplasmic vacuolation, ballooning degeneration as well as enhanced plasma activities of AST and ALT in fish after glyphosate exposure (Cao et al., 2022; Liu et al., 2021). The apparent liver injury was not observed in the current study could be due to low exposure concentrations (<100 μg/L) compared with higher concentrations (>5000 μg/L). However, to further investigate whether glyphosate exposure can cause inflammatory responses, the major proinflammatory cytokines associated with liver inflammation were quantified. In the present study, elevated transcript levels of several proinflammatory markers (e.g., *il-1β*, *il-6*, *tgf-β2* and *tnf-α*) was observed. This result is consistent with significant upregulation inflammatory cytokines (e.g., *il-1β*, *il-6*, *tnf-α*) genes in glyphosate treated common carp (Cao et al., 2022; Liu et al., 2021). Inflammation is frequently stimulated as a secondary response, and plays a critical role in hepatic damage (Jia et al., 2019). These findings validate that hepatic inflammation results from induction of glyphosate exposure in grass carp. Likewise, elevated transcript levels of several proinflammatory cytokines and structural defects were also observed in intestine, indicating glyphosate exposure caused intestinal damage. Our results are also consistent with a previous study showing that glyphosate treatment induced inflammation and histological injury in zebrafish gut

(Ding et al., 2021). In addition to histological examination of intestine, we also measured the content of LPS in the gut and found the concentrations were increased. LPS is a strong inducer of proinflammatory cytokines, and is produced by harmful gut bacteria such as Proteobacteria which showed enriched abundances in our present and previous studies (Yan et al., 2022b). LPS can bind and activate the transmembrane receptor protein to promote the expression of proinflammatory cytokines, which are closely associated with liver injury (Dapito et al., 2012). Due to the direct anatomical connection with the gastrointestinal tract, the liver is constantly exposed to microbial products such as LPS and secondary bile acids, which are closely associated with liver inflammation via the gut–liver axis (Zhang et al., 2022; Zheng et al., 2021). Moreover, the significantly decreased activities of α-amylase and lipase indicated the impairment of intestinal digestive function. Altogether, these results suggested that exposure of glyphosate increased serum LPS level and promoted inflammation in gut and liver (Fig. 7).

4.3. Lipid metabolism alterations

However, hepatic vacuolization is evident in this study. It has been considered as a symptom of steatosis due to lipid accumulation (Guo et al., 2021). We also investigated visceral fat disposition and lipid profiles in serum. Deposition of visceral fat was reduced. The distribution and accumulation of fat are associated with lipid metabolism, and abnormal deposition of visceral fat are valuable clinical indicator of many metabolic diseases (Karpe and Pinnick, 2015). Furthermore, serum lipid parameters were also changed, including increase in TG, and

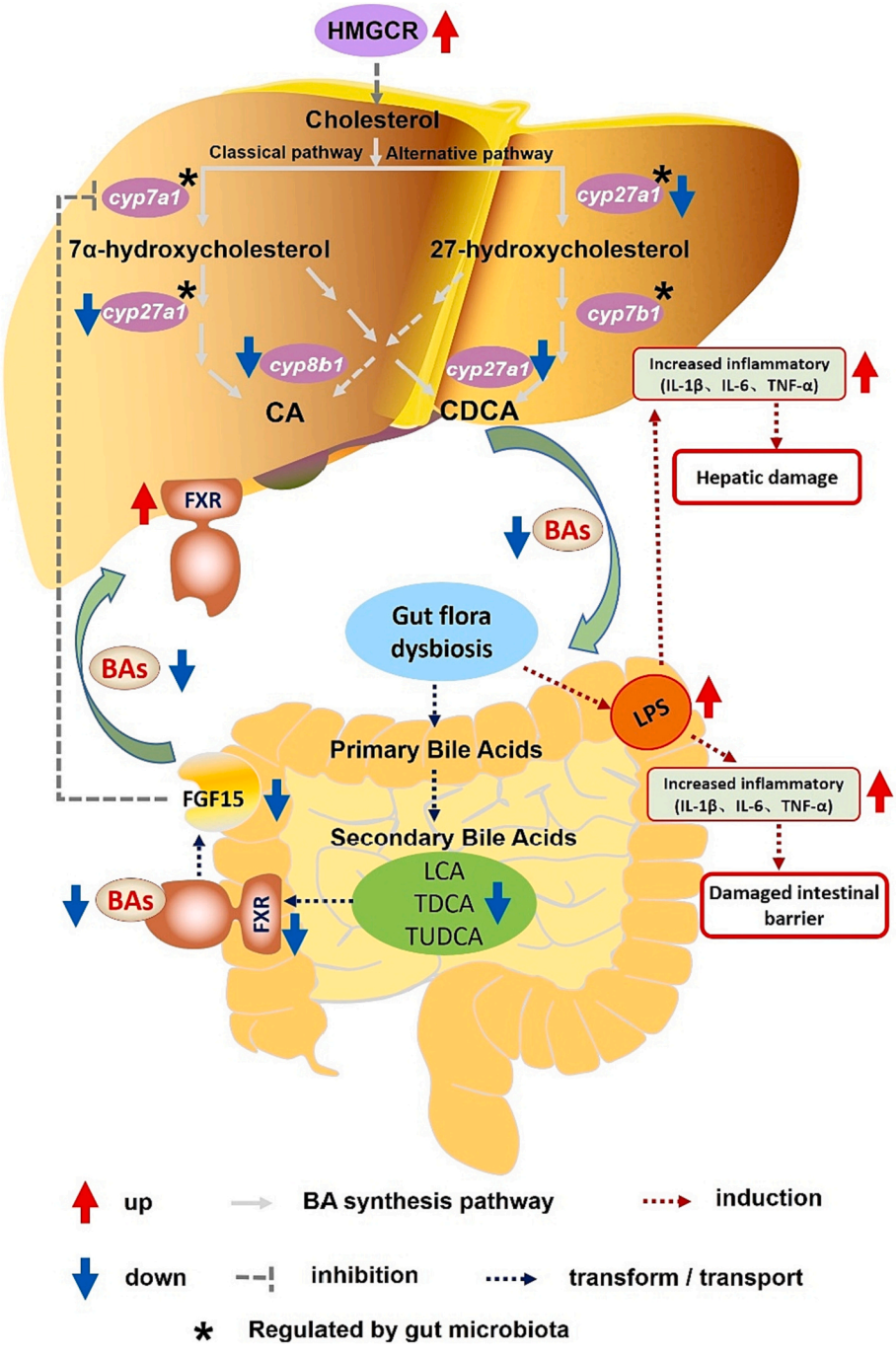

Fig. 7. Schematic depicting the perturbed metabolic pathways along the gut-liver axis after exposure to glyphosate. *cyp7a1*, cholesterol 7α-hydroxylase; *cyp7b1*, oxysterol 7α-hydroxylase; *cyp8b1*, sterol 12α-hydroxylase; *cyp27a1*, sterol 27-hydroxylase; *hmgcr*, 3-hydroxy-3-methylglutaryl-CoA reductase; FGF15, fibroblast growth factors 15; FXR, farnesoid X receptor; CA, cholic acid; CDCA, chenodeoxycholic acid; BAs, bile acids; LCA, lithocholic acid; TDCA, taurodeoxycholic acid; TUDCA, tauroursodeoxycholic acid; LPS, lipopolysaccharide ; IL-1β, interleukin 1 β; IL-6, interleukin 6; TNF-α, tumor necrosis factor α.

reductions in T-CHO, LDL-C and HDL-C. It has been reported that significant elevation of plasma levels of T-CHO, TG, HDL-C in juvenile common carp (Liu et al., 2021). The different responses of lipid parameters may be related to exposure concentrations and exposure time. The altered levels of lipid indicate that glyphosate exposure disturbs normal lipid metabolism in grass carp.

4.4. Disturbance in gut-liver axis

The gut-liver axis is one of the crucial links between the gut microbiota and the extra-intestinal organs, which has important implications for maintaining metabolism health (Blesl and Stadlbauer, 2021; Hu et al., 2021). The liver releases primary bile acids and bioactive mediators into the intestine by biliary tract. In intestine, the host and microorganisms metabolize endogenous (primary bile acids and others) and exogenous (diet and environment) substrates, which translocate to the liver through the portal vein and influence liver functions (Tripathi et al., 2018; Xue et al., 2021). In this study, differential metabolites in liver from glyphosate-exposed fish were related to lipid and bile acids metabolism (Fig. 6A and B). Metabolomics combined with biochemical detection found that glyphosate exposure significantly affected bile acids biosynthesis and decreased total bile acids content in liver (Fig. 4C), which was characterized by significant decreases of the primary (CDCA), conjugated primary (TCA and TCDCA) and secondary bile acids (TDCA and TUDCA) (Fig. 4A). Similarly, the level of bile acids in the intestine was also decreased in response to glyphosate exposure (Fig. 4D).

In order to further confirm that glyphosate exposure changed the biosynthetic pathway of bile acids along the gut-liver axis, the gene transcriptions were examined. For the bile acids synthesis in liver, CYP8B1 is a key enzyme in the synthesis of CA and controls the ratio of CA/CDCA. The key product of CYP8B1, CA, as a major 12-hydroxy (12-OH) bile acids, plays an essential role in promoting absorption of cholesterol by intestine (Xu et al., 2016). Decreased hepatic *cyp27a1* and *cyp8b1* expression, thereby affecting the conversion from cholesterol to CA and resulted in the lower total bile acids level in the liver. Meanwhile, the *hmgcr*, coding the rate-limiting enzyme 3-hydroxy-3-methylglutaryl-CoA reductase (HMGCR) in the hepatic biosynthesis of cholesterol (Cánovas et al., 2010), was also upregulated in this study. The HMGCR reduces blood cholesterol levels and increases liver cholesterol synthesis to maintain normal cholesterol levels in the body (Cánovas et al., 2010; Zhao et al., 2021). The increase of *hmgcr* expression in the liver, which might be a compensatory mechanism to increase the content of cholesterol for bile acids synthesis (Luo et al., 2021). FXR is the most important receptor involved in regulating the enterohepatic circulation and homeostasis of bile acids. FXR also acts as an inhibitor of bile acids synthesis in the liver (Sun et al., 2019), which is related to the regulatory effect of negative feedback of FXR on the de novo synthesis of bile acids (Schmitt et al., 2015). However, in our present study, the glyphosate exposure elevated transcription of hepatic *fxr*, and that was inconsistent with the inhibited enzymes (*cyp27a1* and *cyp8b1*) facilitating hepatic bile acids synthesis. In addition, bile acids concentrations in gut were also reduced in glyphosate-exposed fish. The *fxr* and *fgf15* were both inhibited in the gut, suggesting a disinhibition on the de novo synthesis of bile acids in the liver (Inagaki et al., 2005; Zhang et al., 2020).

For the secondary bile acids in the gut, they are transformed from the conjugated primary bile acids by gut microbes for lipids digestion and absorption (Pathak et al., 2018; Wahlström et al., 2016), as well as for lipid metabolism regulation (Kumari et al., 2020). The gut microbes such as Firmicutes can regulate primary bile acids metabolism by dihydroxylating them into conjugated secondary bile acids (e.g., DCA, UDCA and LCA) (Wahlström et al., 2016; Hu et al., 2021). Here we also observed that the genera *Firmicutes* diminished drastically in the 100 μg/L group by comparing to the control. This is in consistent with the significant reduction of intestinal secondary and total bile acids pool. These evidences indicate that glyphosate exposure disrupted the hepatic synthesis and enterohepatic circulation of bile acids by interfering with the synthetic pathway regulation and gut microbiota composition (Fig. 7), which might lead to the lipid metabolism disorders. Therefore, it could be deduced that the accumulation of glyphosate and AMPA in the intestine caused dysbiosis of the gut microbiota, which led to disrupted bile acids (BAs) metabolism and increased LPS for the gut-liver damage. The intestinal down-regulation of *fxr* and *fgf15* would contribute to the de novo synthesis of BAs in the liver, while the decrease of the circulating BAs might induce up-regulation of HMGCR for a compensation. Glyphosate exposure could also reduce the expression of hepatic *cyp27a1* and *cyp8b1*, which were involved in the conversion of cholesterol to BAs. This could lead to a decrease of the total BAs in the liver and intestine, which would further disrupt lipid metabolism and growth in the exposed fish (Fig. 7). Overall, enriched glyphosate and AMPA in the gut and liver could induce dysregulation of the gut-liver axis through multiple pathways, which ultimately led to lipid metabolism disorders and adverse health effects in non-target organisms.

In conclusion, glyphosate exposure affected the growth of grass carp, reduced visceral fat and caused pathological damage and inflammation to liver and intestine, as well as reduced liver function and increased blood lipid levels. Glyphosate exposure interfered with the physiological functions of the intestinal flora, diminished the *Firmicutes* genera, and further inhibited intestinal *fxr* and *fgf15* genes expression, and resulted in inhibition of the bile acids synthesis of the liver. Exposure to glyphosate also reduced hepatic *cyp27a1* and *cyp8b1* genes expression, which suppressed the conversion of cholesterol to bile acids, and consequently led to the decrease of the total bile acids in the liver and intestine. This in turn might contributed to the disruption of lipid metabolism and growth inhibition in the exposed fish. Collectively, the present study highlights the health hazard of environmental levels of glyphosate exposure posed to aquatic vertebrates by disturbing the gut-liver axis.

CRediT authorship contribution statement

Biao Yan: Investigation, Data curation, Methodology, Formal analysis, Writing – original draft. **Yumiao Sun:** Investigation, Methodology. **Kaiyu Fu:** Investigation, Methodology. **Yindan Zhang:** Investigation, Methodology. **Lei Lei:** Data curation, Formal analysis. **Jun Men:** Methodology, Formal analysis. **Yongyong Guo:** Investigation, Methodology, Formal analysis. **Shengmin Wu:** Conceptualization, Investigation, Writing – review & editing, Funding acquisition, Supervision. **Jian Han:** Conceptualization, Investigation, Writing – review & editing, Funding acquisition, Supervision. **Bingsheng Zhou:** Funding acquisition, Writing – review & editing, Supervision, Project administration.

Declaration of competing interest

The authors declare that they have no known competing financial interests or personal relationships that could have appeared to influence the work reported in this paper.

Data availability

Data will be made available on request.

Acknowledgements

This research was supported by the Open Project of State Environmental Protection Key Laboratory of Pesticide Environmental Assessment and Pollution Control, the National Key Research and Development Program of China (No. 2018YFD0900701), the National Natural Science Foundation of China (No. 22276213) and the State Key Laboratory of Freshwater Ecology and Biotechnology (No. 2022FBZ02).

Appendix A. Supplementary data

Supplementary data to this article can be found online at https://doi.org/10.1016/j.scitotenv.2023.166062.

References

Agency for Toxic Substances and Disease Registry (ATSDR), 2020. Toxicological Profile for Glyphosate. U.S. Department of Health and Human Services, Public Health Service, Atlanta, GA.

Agostini, L.P., Dettogni, R.S., Dos Reis, R.S., Stur, E., Dos Santos, E.V.W., Ventorim, D.P., Garcia, F.M., Cardoso, R.C., Graceli, J.B., Louro, I.D., 2020. Effects of glyphosate exposure on human health: insights from epidemiological and in vitro studies. Sci. Total Environ. 705, 135808.

Annett, R., Habibi, H.R., Hontela, A., 2014. Impact of glyphosate and glyphosate–based herbicides on the freshwater environment. J. Appl. Toxicol. 34, 458–479.

Blesl, A., Stadlbauer, V., 2021. The gut-liver axis in cholestatic liver diseases. Nutrients 13, 1018–1051.

Campana, A.M., Laue, H.E., Shen, Y., Shrubsole, M.J., Baccarelli, A.A., 2022. Assessing the role of the gut microbiome at the interface between environmental chemical exposures and human health: current knowledge and challenges. Environ. Pollut. 315, 120380.

Cánovas, A., Quintanilla, R., Gallardo, D., Díaz, I., Noguera, J.L., Ramírez, O., Pena, R.N., 2010. Functional and association studies on the pig HMGCR gene, a cholesterol-synthesis limiting enzyme. Animal 4, 224–233.

Cao, X., Rao, C., Cui, H., Sun, D., Li, L., Guo, S., Zhou, J., Yuan, R., Yang, S., Chen, J., 2022. Toxic effects of glyphosate on the intestine, liver, brain of carp and on epithelioma papulosum cyprinid cells: evidence from in vivo and in vitro research. Chemosphere 302, 134691.

Chen, J., Rao, C., Yuan, R., Sun, D., Guo, S., Li, L., Yang, S., Qian, D., Lu, R., Cao, X., 2022. Long-term exposure to polyethylene microplastics and glyphosate interferes with the behavior, intestinal microbial homeostasis, and metabolites of the common carp (*Cyprinus carpio*). Sci. Total Environ. 814, 152681.

Clements, D., Dugdale, T.M., Butler, K.L., Florentine, S.K., Sillitoe, J., 2017. Herbicide efficacy for aquatic Alternanthera philoxeroides management in an early stage of invasion: integrating above-ground biomass, below-ground biomass and viable stem fragmentation. Weed Res. 57, 257–266.

Dapito, D.H., Mencin, A., Gwak, G.Y., Pradere, J.P., Jang, M.K., Mederacke, I., Caviglia, J.M., Khiabanian, H., Adeyemi, A., Bataller, R., Lefkowitch, J.H., Bower, M., Friedman, R., Sartor, R.B., Rabadan, R., Schwabe, R.F., 2012. Promotion of hepatocellular carcinoma by the intestinal microbiota and TLR4. Cancer Cell 21 (4), 504–516.

Dey, S., Samanta, P., Pal, S., Mukherjee, A.K., Kole, D., Ghosh, A.R., 2016. Integrative assessment of biomarker responses in teleostean fishes exposed to glyphosate-based herbicide (Excel Mera 71). Emerg. Contaminant. 2, 191–203.

Ding, W., Shangguan, Y., Zhu, Y., Sultan, Y., Feng, Y., Zhang, B., Liu, Y., Ma, J., Li, X., 2021. Negative impacts of microcystin-LR and glyphosate on zebrafish intestine: linked with gut microbiota and microRNAs? Environ. Pollut. 286, 117685.

Evariste, L., Barret, M., Mottier, A., Mouchet, F., Gauthier, L., Pinelli, E., 2019. Gut microbiota of aquatic organisms: a key endpoint for ecotoxicological studies. Environ. Pollut. 248, 989–999.

Fantón, N., Cazenave, J., Michlig, M.P., Repetti, M.R., Rossi, A., 2021. Biomarkers of exposure and effect in the armoured catfish Hoplosternum littorale during a rice production cycle. Environ. Pollut. 287, 117356.

Geng, Y., Jiang, L., Zhang, D., Liu, B., Zhang, J., Cheng, H., Wang, L., Peng, Y., Wang, Y., Zhao, Y., Xu, Y., Liu, X., 2021. Glyphosate, aminomethylphosphonic acid, and glufosinate ammonium in agricultural groundwater and surface water in China from 2017 to 2018: occurrence, main drivers, and environmental risk assessment. Sci. Total Environ. 769, 144396.

Giommi, C., Ladisa, C., Carnevali, O., Maradonna, F., Habibi, H.R., 2022. Metabolomic and transcript analysis revealed a sex-specific effect of glyphosate in zebrafish liver. Int. J. Mol. Sci. 23, 2724.

Glusczak, L., Miron, D.D.S., Crestani, M., Fonseca, M.B.D., Pedron, F.D.A., Duarte, M.F., Vieira, V.L.P., 2006. Effect of glyphosate herbicide on acetylcholinesterase activity and metabolic and hematological parameters in piava (*Leporinus obtusidens*). Ecotoxicol. Environ. Saf. 65, 237–241.

Guo, W., Lei, L., Shi, X., Li, R., Wang, Q., Han, J., Yang, L., Chen, L., Zhou, B., 2021. Nonalcoholic fatty liver disease development in zebrafish upon exposure to bis(2-ethylhexyl)-2,3,4,5-tetrabromophthalate, a novel brominated flame retardant. Environ. Sci. Technol. 55, 6926–6935.

Hu, C., Liu, M., Wan, T., Tang, L., Sun, B., Zhou, B., Lam, J.C.W., Lam, P.K.S., Chen, L., 2021. Disturbances in microbial and metabolic communication across the gut–liver axis induced by a dioxin-like pollutant: an integrated metagenomics and metabolomics analysis. Environ. Sci. Technol. 55, 529–537.

Inagaki, T., Choi, M., Moschetta, A., Peng, L., Cummins, C.L., McDonald, J.G., Luo, G., Jones, S.A., Goodwin, B., Richardson, J.A., Gerard, R.D., Repa, J.J., Mangelsdorf, D. J., Kliewer, S.A., 2005. Fibroblast growth factor 15 functions as an enterohepatic signal to regulate bile acid homeostasis. Cell Metab. 2, 217–225.

Jia, R., Du, J., Cao, L., Li, Y., Johnson, O., Gu, Z., Jeney, G., Xu, P., Yin, G., 2019. Antioxidative, inflammatory and immune responses in hydrogen peroxide-induced liver injury of tilapia (GIFT, *Oreochromis niloticus*). Fish Shellfish Immunol. 84, 894–905.

Karpe, F., Pinnick, K.E., 2015. Biology of upper-body and lower-body adipose tissue–link to whole-body phenotypes. Nat. Rev. Endocrinol. 11 (2), 90–100.

Kumari, A., Pal Pathak, D., Asthana, S., 2020. Bile acids mediated potential functional interaction between FXR and FATP5 in the regulation of lipid metabolism. Int. J. Biol. Sci. 16, 2308–2322.

Li, M.H., Ruan, L.Y., Zhou, J.W., Fu, Y.H., Jiang, L., Zhao, H., Wang, J.S., 2017. Metabolic profiling of goldfish (*Carassius auratis*) after long-term glyphosate-based herbicide exposure. Aquat. Toxicol. 188, 159–169.

Liu, J., Dong, C., Zhai, Z., Tang, L., Wang, L., 2021. Glyphosate-induced lipid metabolism disorder contributes to hepatotoxicity in juvenile common carp. Environ. Pollut. 269, 116186.

Luo, G., Li, Z., Lin, X., Li, X., Chen, Y., Xi, K., Xiao, M., Wei, H., Zhu, L., Xiang, H., 2021. Discovery of an orally active VHL-recruiting PROTAC that achieves robust HMGCR degradation and potent hypolipidemic activity *in vivo*. Acta Pharm. Sin. B 11 (5), 1300–1314.

Pathak, P., Xie, C., Nichols, R.G., Ferrell, J.M., Boehme, S., Krausz, K.W., Patterson, A.D., Gonzalez, F.J., Chiang, J.Y.L., 2018. Intestine farnesoid X receptor agonist and the gut microbiota activate G-protein bile acid receptor-1 signaling to improve metabolism. Hepatology 68, 1574–1588.

Sabio, Y., García, C.A., Vera, M.S., Vinocur, A., Graziano, M., Miranda, C., Pizarro, H.N., 2022. Rethinking the term "glyphosate effect" through the evaluation of different glyphosate-based herbicide effects over aquatic microbial communities. Environ. Pollut. 292, 118382.

Sakashita, M., Sato, M., Kondo, S., 2019. Comparative morphological examination of vertebral bodies of teleost fish using high-resolution micro-CT scans. J. Morphol. 280, 778–795.

Schmitt, J., Kong, B., Stieger, B., Tschopp, O., Schultze, S.M., Rau, M., Weber, A., Müllhaupt, B., Guo, G.L., Geier, A., 2015. Protective effects of farnesoid X receptor (FXR) on hepatic lipid accumulation are mediated by hepatic FXR and independent of intestinal FGF15 signal. Liver Int. 35 (4), 1133–1144.

Shiogiri, N.S., Paulino, M.G., Carraschi, S.P., Baraldi, F.G., da Cruz, C., Fernandes, M.N., 2012. Acute exposure of a glyphosate-based herbicide affects the gills and liver of the Neotropical fish, *Piaractus mesopotamicus*. Environ. Toxicol. Pharmacol. 34, 388–396.

Solomon, K.R., Thompson, D.G., 2003. Ecological risk assessment for aquatic organisms from over-water uses of glyphosate. J. Toxicol. Environ. Health B Crit. Rev. 6, 289–324.

Sun, L., Pang, Y., Wang, X., Wu, Q., Liu, H., Liu, B., Liu, G., Ye, M., Kong, W., Jiang, C., 2019. Ablation of gut microbiota alleviates obesity-induced hepatic steatosis and glucose intolerance by modulating bile acid metabolism in hamsters. Acta Pharm. Sin. B 9 (4), 702–710.

Szarek, J., Siwicki, A., Andrzejewska, A., Terech-Majewska, E., Banaszkiewicz, T., 2000. Effects of the herbicide roundup on the ultrastructural pattern of hepatocytes in carp (*Cyprinus carpio*). Mar. Environ. Res. 50, 263–266.

Tripathi, A., Debelius, J., Brenner, D.A., Karin, M., Loomba, R., Schnabl, B., Knight, R., 2018. The gut-liver axis and the intersection with the microbiome. Nat. Rev. Gastroenterol. Hepatol. 15, 397–411.

Van Bruggen, A.H.C., He, M.M., Shin, K., Mai, V., Jeong, K.C., Finckh, M.R., Morris, J.G., 2018. Environmental and health effects of the herbicide glyphosate. Sci. Total Environ. 616-617, 255–268.

Villamar-Ayala, C.A., Carrera-Cevallos, J.V., Vasquez-Medrano, R., Espinoza-Montero, P. J., 2019. Fate, eco-toxicological characteristics, and treatment processes applied to water polluted with glyphosate: a critical review. Crit. Rev. Environ. Sci. Technol. 49, 1476–1514.

Wahlström, A., Sayin, S.I., Marschall, H.U., Bäckhed, F., 2016. Intestinal crosstalk between bile acids and microbiota and its impact on host metabolism. Cell Metab. 24, 41–50.

Xu, Y., Li, F., Zalzala, M., Xu, J., Gonzalez, F.J., Adorini, L., Lee, Y.K., Yin, L., Zhang, Y., 2016. Farnesoid X receptor activation increases reverse cholesterol transport by modulating bile acid composition and cholesterol absorption in mice. Hepatology 64, 1072–1085.

Xue, R., Su, L., Lai, S., Wang, Y., Zhao, D., Fan, J., Chen, W., Hylemon, P.B., Zhou, H., 2021. Bile acid receptors and the gut-liver axis in nonalcoholic fatty liver disease. Cells 10, 2806–2824.

Yan, B., Lei, L., Chen, X., Men, J., Sun, Y., Guo, Y., Yang, L., Wang, Q., Han, J., Zhou, B.S., 2022a. Glyphosate and glufosinate-ammonium in aquaculture ponds and aquatic products: occurrence and health risk assessment. Environ. Pollut. 296, 118742.

Yan, B., Han, J., Sun, Y., Lei, L., Yuan, J., Qiao, Z., Men, J., Wang, X., Guo, Y., Wang, Q. D., Zhou, B.S., 2022b. Probiotics ameliorate growth retardation of glyphosate by regulating intestinal microbiota and metabolites in crucian carp (*Carassius auratus*). Sci. Total Environ. 851, 158260.

Zhang, C., Feng, L., He, T.T., Yang, C.H., Chen, G.Q., Tian, X.S., 2015. Investigating the mechanisms of glyphosate resistance in goosegrass (*Eleusine indica*) population from South China. J. Integr. Agric. 14, 909–918.

Zhang, S., Xu, J., Kuang, X., Li, S., Li, X., Chen, D., Zhao, X., Feng, X., 2017. Biological impacts of glyphosate on morphology, embryo biomechanics and larval behavior in zebrafish (*Danio rerio*). Chemosphere 181, 270–280.

Zhang, C., Wang, Z., Feng, Q., Chen, W.D., Wang, Y.D., 2020. Farnesoid X receptor: a potential therapeutic target in multiple organs. Histol. Histopathol. 35, 1403–1414.

Zhang, P., Zheng, L., Duan, Y., Gao, Y., Gao, H., Mao, D., Luo, Y., 2022. Gut microbiota exaggerates triclosan-induced liver injury via gut-liver axis. J. Hazard. Mater. 421, 126707.

Zhao, X., Xu, J., Tang, X., Huang, K., Li, J., Liu, R., Jiang, L., Zhang, Y., Wang, D., Sun, K., Xu, B., Zhao, W., Hui, R., Gao, R., Song, L., Yuan, J., 2021. Effect of NPC1L1 and HMGCR genetic variants with premature triple-vessel coronary disease. Front Cardiovasc Med. 8, 704501.

Zheng, T., Jia, R., Cao, L., Du, J., Gu, Z., He, Q., Xu, P., Yin, G., 2021. Effects of chronic glyphosate exposure on antioxdative status, metabolism and immune response in

tilapia (GIFT, *Oreochromis niloticus*). Comp. Biochem. Physiol. C Toxicol. Pharmacol. 239, 108878.
Zhou, L., Limbu, S.M., Qiao, F., Du, Z.Y., Zhang, M., 2018. Influence of long-term feeding antibiotics on the gut health of zebrafish. Zebrafish 15, 340–348.
Zhou, Y., Guo, W., Lei, L., Sun, Y., Li, R., Guo, Y., Yang, L., Shi, X., Han, J., Zhou, B., 2021. Bis(2-ethylhexyl)-tetrabromophthalate induces zebrafish obesity by altering the brain-gut axis and intestinal microbial composition. Environ. Pollut. 290, 118127.